

# PROPAGATION CHARACTERISTICS OF LIGHTNING-GENERATED WHISTLERS IN THE JOVIAN MAGNETOSPHERE AND LIGHTNING ACTIVITY

Yasuhide Hobara, Sei Kanemaru and Masashi Hayakawa  
Department of Electric Engineering,  
The University of Electro-Communications, Chofu Tokyo 182, Japan

## 1 Introduction

Strong evidence of lightning on Jupiter comes from the Voyager observations of whistlers [Gurnett *et al.*, 1979; Kurth *et al.*, 1985] just like the terrestrial whistlers. In the previous studies, emphasis was primarily placed on the observed dispersion characteristics of whistlers. However, in order to understand all other important characteristics of whistlers (their amplitude, its frequency dependence) and then to deduce the properties of the causative lightning (i.e., discharge intensity, occurrence frequency, source frequency spectra, etc.), we have to make full use of the amplitude information. In this paper, we will estimate the total decrease (and/or increase) of the wave amplitude due to the polarization effect, focusing/defocusing and collisionless (Landau and cyclotron) damping during the course of magnetospheric propagation. These theoretical predictions are compared with the experimental data by the Voyager spacecraft, in order to study the properties of causative lightning and electron density distribution of the magnetosphere.

## 2 Lightning Whistler in the Jovian Magnetosphere

We have reexamined the Voyager-1 wideband waveform data especially to focus on the amplitude information of the lightning whistlers. About 90 whistlers have been examined to determine the dispersion and upper and lower cutoff frequencies among three different representative regions the so-called A, B and C regions [Kurth *et al.*, 1985]. Most whistlers are very weak and only 28 whistlers are strong enough to derive their frequency spectra as an amplitude information.

The number of the whistlers used in the region A is two, while there are 15 and 11 events respectively for B and C. The average dispersion in the region B is smallest (about 70 sec Hz<sup>1/2</sup>). Larger dispersion values are observed at other two regions (i.e. about 280 sec Hz<sup>1/2</sup> for A and about 450 sec Hz<sup>1/2</sup> for C). These results are in a good agreement with the previous results [Kurth *et al.*, 1985]. Both the observed dispersions and high- and low-frequency cutoffs have been used as one of the initial conditions for two-dimensional ray-tracing computations to determine the propagation path of whistlers from the Jovian ionosphere toward the Voyager-1 spacecraft.

An example of the traced whistler peaks is shown in Fig. 3. The whistler signals are generally very weak (about 10 dB larger than the noise level), such that 60 m sec average frequency spectra are noisy as well. Thus, the detection of a whistler signal is highly dependent on the regions where whistler activity was detected and could be determined by the variations of receiver sensitivity due to changes in the background broadband signal strength [Kurth *et al.*, 1985]. Note that the trend of the noise is different among the three regions. That is, the intensity of noise in A and C is rather big (around 10<sup>-12</sup> V<sup>2</sup>m<sup>-2</sup>Hz<sup>-1</sup> and 10<sup>-13</sup> V<sup>2</sup>m<sup>-2</sup>Hz<sup>-1</sup>, respectively) compared to the value in B (~10<sup>-14</sup> V<sup>2</sup>m<sup>-2</sup>Hz<sup>-1</sup>). This variation is proportional to the whistler dispersion and also to the cold plasma density. We can show the average whistler absolute power spectrum density with an error bar of one standard deviation in Fig. 1. Average power spectrum density over the region B is smaller and about 10<sup>-12.5</sup> V<sup>2</sup>m<sup>-2</sup>Hz<sup>-1</sup>, while the average spectrum density is around 10<sup>-11</sup> V<sup>2</sup>m<sup>-2</sup>Hz<sup>-1</sup> and 10<sup>-12</sup> V<sup>2</sup>m<sup>-2</sup>Hz<sup>-1</sup>, respectively, at A and C.

### 3 Determination of Total Wave Amplitude Decrease

In this paper we have performed the first attempt to carry out the ray-tracing computations, taking into account the amplitude of the wave field, the details of which are described in *Molchanov et al.*, [1995]. The essential point of the method is to compute the variation of electric and magnetic field amplitude caused by the changes in wave polarization (coefficient.  $K_{pe}$ ), focusing/defocusing ( $K_f$ ) and kinetic collisionless damping ( $K_a$ ) along the ray trajectory by using the continuity of Poynting flux along the path. For simplicity, we adopt a two-dimensional ray-tracing procedure. The essential and necessary characteristics of the computational procedure are summarized below.

1. Polarization coefficient;  $K_{pe} = (K_{e0}/K_e)(\sqrt{n_0/n})$ . During the course of propagation, the wave will suffer from the change in polarization (for the electric field), and this effect can be characterized by the following equation [*Molchanov et al.*, 1995]:

$$K_e = \frac{1}{(1 + \rho^2 + \rho_z^2)^{\frac{1}{2}}} \times \{[\sin\theta(\rho^2 + \rho_z^2) - \rho_z \cos\theta]^2 + [\cos\theta(1 + \rho^2) - \rho_z \sin\theta]^2\}^{\frac{1}{4}} \quad (1)$$

where  $\rho = -i(E_y/E_x)$  and  $\rho_z = E_z/E_x$  are wave polarizations.  $\theta$  is the wave normal angle, and  $K_{e0}:K_e$  at the initial point of the ray trajectory and the refractive index  $n_0:n$  at the initial point of the trajectory. The axis  $z$  is assumed to be parallel to the Jovian magnetic field, and the wave normal direction making an angle  $\theta$  with  $z$  axis.

2. Focusing /defocusing coefficient  $K_f$ . The focusing and defocusing effect can be found by comparing the paths of adjacent rays.

$$K_f = \sqrt{\frac{S_0}{S}} \quad (2)$$

where  $S$  and  $S_0$  are the cross sections of a flux tube respectively at an arbitrary and the initial point of the trajectory.

3. Damping (amplification) coefficient:  $K_a = \exp(-\int_0^\tau \gamma d\tau)$ . We have to consider the collisionless wave damping. We can suppose a bi-Maxwellian velocity distribution for the magnetospheric particles as follows.

$$f_0 = \frac{N_e}{\pi^{\frac{3}{2}} v_{T\parallel} v_{T\perp}^2} e^{-\left(\frac{v_{\parallel}^2}{v_{T\parallel}^2} + \frac{v_{\perp}^2}{v_{T\perp}^2}\right)} \quad (3)$$

where  $v_{T\parallel} = (2\kappa T_{\parallel}/m_e)^{\frac{1}{2}}$ ,  $v_{T\perp} = (2\kappa T_{\perp}/m_e)^{\frac{1}{2}}$  ( $v_{T\parallel}$  and  $v_{T\perp}$  are the parallel and perpendicular components of electron thermal velocity), and  $a = T_{\perp}/T_{\parallel}$  is the temperature anisotropy. For this general electron distribution function, we can derive the following formula of attenuation due to wave particle interactions:

$$\gamma = -\frac{\sqrt{\pi}\omega_{pe}^2}{2\omega n n_{g\parallel}} b a_x^2 \left[ p_0 e^{-b^2 \kappa^2} + p_1 e^{-b^2(1-\kappa^2)} \right] \quad (4)$$

where

$$p_0 = 2\kappa \left[ \frac{a^2}{2b^2} \rho^2 \tan^2\theta + b^2 \kappa^2 \rho_z^2 - a \rho \rho_z \kappa \tan\theta \right],$$

$$p_1 = [(1 + \rho)^2 + 2\rho_z(1 + \rho) \tan\theta(\kappa - 1)] [1 - a(1 - \kappa)] + \rho_z^2(1 - \kappa)^2 \tan^2\theta a [\kappa - (1 - a)],$$

$$b = \frac{c}{v_{T\parallel} \kappa n \cos\theta}, \quad \kappa = \frac{\omega}{\omega_{ce}}, \quad a_x^2 = (1 + \rho + \rho_z^2)^{-1}$$

and  $n_{g\parallel}$  is the parallel component of group refractive index of cold plasma. In the above equation,

the first term indicates Landau damping, while the second term, cyclotron damping. Both types of damping depend strongly on the particle distribution function.

We have used a centered dipole field model for the Jovian magnetic field, with an equatorial electron gyrofrequency of 11700 kHz on the surface (the surface is assumed to be a height of 1 bar). The cold plasma density profile in the magnetosphere and Io plasma torus was originally based on the model by *Divine et al.* [1983]. We have modified the density profile such that we add a certain amount of the density increase uniformly to all the regions just like a bias (we call it “offset” in the following) to have the rays to reach the Voyager spacecraft. The effect of this bias appears only in the upper cutoff frequency and has almost no influence on the amplitude attenuation [*Hobara et al.*, 1995]. The ray-tracing computations have been carried out for each 48 second PWS wideband frame data for which the lightning whistlers were detected. Fig. 2 illustrates the expected total decrease of wave electric field as a function of the electron temperature at the Voyager in one example of the events in the region A, which indicates a decrease of at least 40 dB for any electron temperatures. Also this amount of decrease remains nearly constant over the most of the observed frequency range. Average total decrease within each representative region has been derived as 37 dB for A and 29 dB and 33.25 dB for B and C, respectively. According to our ray-tracing calculations on the assumption of unducted propagation, most of the observed lightning-generated whistlers in all three regions originate from higher latitudes  $\sim 60^\circ$ , and so they would suffer from a transmission loss of only a few dB within the ionosphere [*Nagai et al.*, 1993 Hayakawa . 1995 ].

## 4 Estimated Properties of Jovian Lightning

By using the theoretical estimation in the previous section, Fig. 3 illustrates one example of whistler frequency spectra and that of its estimated causative lightning. Solid curve represents the observed whistler peak, which suggests.

$$P_{\text{lightning}} \propto f^{-2} \quad (5)$$

where  $P_{\text{lightning}}$  is the deduced power spectral density of the causative lightning in the VLF range at the bottom of the Jovian ionosphere. Fig. 3 suggests that the frequency spectrum is rather smooth in most part, which may imply that a possibility of the existence of the ionospheric ledges is very small. The Poynting flux at the bottom of Jovian ionosphere from the lightning flash can be estimated by using the total decrease factor in the previous section, and then the total radiation power from the Jovian lightning flash in the radio frequency range (0~20 kHz) is estimated. Fig. 4 illustrates the total radiated power of the lightning per flash as a function of time. Average radiation power in B is  $10^{2.5}$  W, and  $10^5$  W at C. We have obtained the largest value of  $10^6$  W at A, but its reliability is a problem because of only two events. So, the relative difference in power at the different regions are mainly controlled by the spectral density of whistlers rather than the propagation loss.

## 5 Conclusion

1. The first attempt of ray-tracing computations taking into account the amplitude information is made full use of in estimating the lightning characteristics in Jupiter.
2. Calculated total radiation power of amplitude of whistlers in the region B is smaller and about 29 dB, while  $\sim 37$  dB and  $\sim 33$  dB in A and C respectively.
3. Estimated the individual frequency spectrum of the causative lightning shows that its intensity is roughly proportional to the inverse square of the frequency in the VLF range. And the smoothness of this variation may imply a small possibility of the existence of the ionospheric ledges.

4. Average total radiation power of the lightning in VLF range (0~20 kHz) has been derived, as  $10^{2.5}$  W in the region B,  $10^6$  W and  $10^5$  W in A and C respectively. These values are in the range of the terrestrial case ( $\sim 10^5$  W in the same frequency range), which suggest that the lightning activity in Jupiter is comparable to the terrestrial case in the sense of their radiation power.

## References

- Divine, N., and H.B. Garrett, Charged particle distributions in Jupiter's magnetosphere, *J. Geophys. Res.*, **88**, 6889, 1983.
- Gurnett, D.A., R.R. Shaw, R.R. Anderson, W.S. Kurth, and F.L. Scarf, Whistlers observed by Voyager 1: Detection of lightning on Jupiter, *Geophys. Res. Lett.*, **6**, 511, 1979.
- Hayakawa, M., Association of whistlers with lightning discharges on the Earth and Jupiter, *J. Atmos. Terr. Phys.*, **57**, 525, 1995.
- Hobara, Y., O.A. Molchanov, M. Hayakawa, and K. Ohta, Propagation characteristics of whistler waves in the Jovian ionosphere and magnetosphere, *J. Geophys. Res.*, **100**, 23523, 1995.
- Kurth, W.S., B.D. Strayer, D.A. Gurnett, and F.L. Scarf, A summary of whistlers observed by Voyager 1 at Jupiter, *Icarus*, **61**, 497, 1985.
- Molchanov, O.A., O.A. Maltseva, Y. Hobara, and M. Hayakawa A new ray tracing technique of VLF wave propagation in the Earth's magnetosphere, *Radio Sci.*, **30**, 1599, 1995.
- Nagai, K., K. Ohta, Y. Hobara, and M. Hayakawa, Transmission characteristics of VLF/ELF radio waves through the Jovian ionosphere, *Geophys. Res. Lett.*, **20**, 22, 1993.

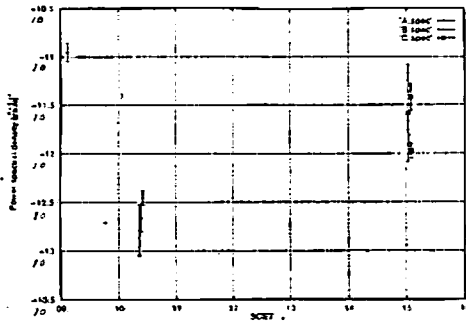


Fig. 1 The average power spectral density of whistlers versus time

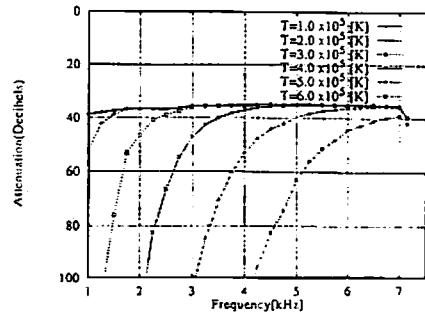


Fig. 2 The expected total decrease in wave electric field as a function of electron temperature at the Voyager in one of the events in the region A

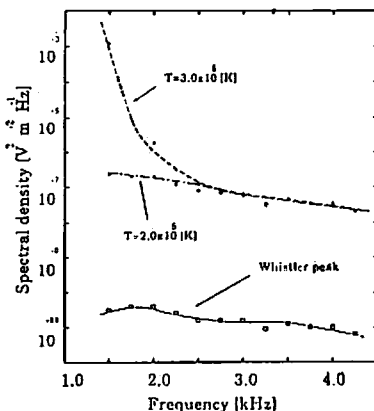


Fig. 3 One example of frequency spectra of a whistler and the corresponding spectra of its causative lightning

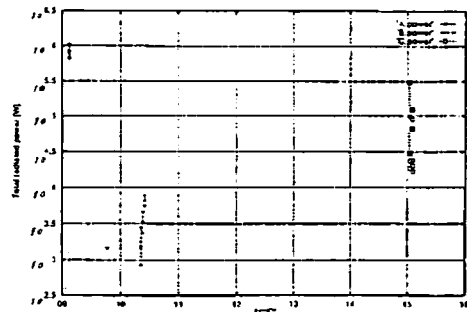


Fig. 4 The total radiation power of Jovian lightning per flash in the frequency range of 0 ~ 20 kHz as a function of time